Int. J. Heat Mass Transfer. Vol 32, No 3, pp. 563–574, 1989
Printed in Great Britain

0017–9310/89 $3.00+0.00
Pergamon Press plc

Fluid flow and heat transfer in an axially rotating pipe—II. Effect of rotation on laminar pipe flow

G. REICH, B. WEIGAND and H. BEER

Institut für Technische Thermodynamik, Technische Hochschule Darmstadt, Petersenstrasse 30, 6100 Darmstadt, Federal Republic of Germany

(*Received* 11 *May* 1988)

Abstract—The effects of tube rotation on the velocity and temperature distribution, on the friction coefficient and on the heat transfer to a fluid flowing laminar inside a tube are examined by analysis. It is demonstrated that the rotation has a destabilizing effect on a laminar pipe flow, which changes to turbulent flow. Free convection vortices, that occur, if the pipe wall is heated, disappear with a growing rotation velocity of the tube. For that purpose a perturbation calculation is performed. By the results of this calculation the disappearance of the free convection vortices is demonstrated evidently.

1. INTRODUCTION

THE STABILITY of isothermal laminar pipe flow with superimposed rotation has been investigated by several authors. By solution of the perturbation equations Pedley [1] demonstrated, that a cylindrically symmetric shear flow of an incompressible fluid, such as Hagen–Poiseuille flow in a circular pipe, is unstable to infinitesimal, inviscid disturbances if it is subjected to a rotation about its axis. These results have been confirmed experimentally by Nagib *et al.* [2]. Mackrodt [3] examined the stability of Hagen–Poiseuille flow with superimposed rigid body rotation against three-dimensional disturbances. By numerical solution of the perturbation equations limiting values of the flow-rate Reynolds number, $Re = 165.76$, and the rotational Reynolds number, $Re_\phi = 53.92$, were calculated, above which the flow becomes unstable. By experiments and by use of a modified mixing length theory Kikuyama *et al.* [4] found a destabilizing effect of rotation on laminar pipe flow. Reference [5] expanded this mixing length model to calculate the fluid flow and heat transfer in an axially rotating pipe with constant wall heat flux.

If the wall of a non-rotating horizontal pipe, submitted to a small flow rate, is heated, already small temperature variations in the fluid cause a secondary flow due to buoyancy forces. Morton [6] investigated this phenomenon and obtained solutions for the velocity and temperature field. This treatment was restricted to small rates of heating, which corresponds to a small ratio of buoyancy and inertia forces, $Gr/Re^2 \ll 1$, so that the motion due to buoyancy could be regarded as secondary flow. Del Casal and Gill [7] expanded this solution for flows with axial density variations. Futayami and Mori [8] investigated the laminar mixed convection in a horizontal pipe for ratios of $Gr/Re^2 \approx 1$ by means of an integral method. Reference [5] observed the formation of convection cells in a heated pipe at low flow rates and high temperature differences, at ratios of $Gr/Re^2 \approx 0.02$. Rotation of the tube about its own axis caused a disappearance of the convection cells, already at a low rotational speed.

In the first part of this paper the effect of rotation on the velocity and temperature distribution, on the friction coefficient and on the heat transfer to a fluid flowing inside a rotating pipe, without free convection, is investigated. In the second part the interaction between free convection effects and rotation is considered.

2. EFFECT OF ROTATION, IF THERMAL BUOYANCY FORCES ARE DISREGARDED

A systematic study on the effect of rotation on the velocity and temperature distribution, on the friction coefficient and on the heat transfer to a fluid flowing inside a tube was carried out in ref. [9], if the flow is initially turbulent. This model is applied in order to demonstrate the effect of rotation on laminar pipe flow. To describe the destabilizing effect on laminar pipe flow the turbulence model is modified.

2.1. *Mathematical formulation*

Since a detailed description of the mathematical model is given in ref. [9], only the most important equations and particularly the modifications of the turbulence model are summarized.

For fully developed flow conditions and for an incompressible fluid the conservation equations in cylindrical coordinates, as illustrated in Fig. 1, take the

NOMENCLATURE

B_i complex constants, $i = 1, \ldots, 6$
C_i constants, $i = 1, \ldots, 6$
c_p specific heat at constant pressure
D pipe diameter
D_i complex constants, $i = 1, \ldots, 6$
d_{iR} real constants which are the real parts of the D_i's, $i = 1, \ldots, 6$
d_{iI} real constants which are the imaginary parts of the D_i's, $i = 1, \ldots, 6$
E Eulerian constant
E_i complex constants, $i = 1, \ldots, 9$
e_{iR} real constants which are the real parts of the E_i's, $i = 1, \ldots, 9$
e_{iI} real constants which are the imaginary parts of the E_i's, $i = 1, \ldots, 9$
f_i functions of $\tilde{r}$, $i = 1, \ldots, 4$
Gr Grashof number, $\beta g \Delta T D^3/\nu^2$
i imaginary unit
J_1 Bessel function
k thermal conductivity
K_ν, L_ν terms of a sum
L pipe length
l, l_q hydrodynamic and thermal mixing length in the rotating pipe
l_0, l_{q0} hydrodynamic and thermal mixing length in the non-rotating pipe
m_0, m_1, m_2 coefficients of the temperature distribution $\tilde{\theta}_0$
n_0, n_1, n_2 coefficients of the axial velocity distribution $\tilde{v}_{z0}$
N rotation rate, Re_ϕ/Re
Nu Nusselt number, $D\,\partial T/\partial r(r = R)/(T_w - T_b)$
Pr Prandtl number, ν/a
Pr_t turbulent Prandtl number, l_0/l_{q0}
p pressure
p' pressure fluctuation
$\tilde{p}^*$ dimensionless time-mean pressure
$\dot{q}$ heat flux density
$\dot{q}_{rw}$ heat flux density at the pipe wall
R pipe radius
Re Reynolds number, $\bar{v}_z D/\nu$
Re_ϕ rotational Reynolds number, $v_{\phi w} D/\nu$
Re_* Reynolds number based on the friction velocity, $v_* R/\nu$
$\tilde{r}$ dimensionless coordinate in radial direction
T time-mean temperature
T' temperature fluctuation
T_w time-mean temperature of the wall
T_b bulk temperature
T_0 time-mean temperature in the centre of the pipe
$v_{ri}, v_{\phi i}, v_{zi}$ time-mean velocity in the radial, tangential, and axial directions, $i = 0, 1, 2$
$\tilde{v}_{ri}, \tilde{v}_{\phi i}, \tilde{v}_{zi}$ dimensionless time-mean velocity in the radial, tangential, and axial directions, $i = 0, 1, 2$
$\tilde{v}_i^*$ dimensionless velocity components, $i = r, \phi, z$
$v_{\phi w}$ tangential velocity of the pipe wall
v_i' velocity fluctuation
$\bar{v}_z$ mean-axial velocity over the pipe cross-section
U, V, W complex functions
Y_1 Weber function
Y^+ dimensionless radial distance from the pipe wall
z coordinate in the axial direction
$\tilde{z}$ dimensionless coordinate in the axial direction.

Greek symbols
δ complex coordinate in the radial direction
ε perturbation parameter, Gr/Re^2
$\theta, \tilde{\theta}, \tilde{\theta}^*$ dimensionless temperature
$\tilde{\theta}'$ dimensionless temperature fluctuation
λ coefficient of friction loss
μ dynamic viscosity
μ_t turbulent dynamic viscosity
ν kinematic viscosity
ρ density
τ_{ij} shear stress
ϕ coordinate in the tangential direction
ψ stream function.

form:

axial momentum equation

$$0 = -\frac{\partial p}{\partial z} + \frac{1}{r}\frac{\partial}{\partial r}(r\tau_{rz}); \tag{1}$$

energy equation

$$\rho c_p v_z \frac{\partial T}{\partial z} = -\frac{1}{r}\frac{\partial}{\partial r}(r\dot{q}_r). \tag{2}$$

For a newtonian fluid with constant properties the shear stress τ_{rz} and the radial component of the heat flux vector can be written as

$$\tau_{rz} = \mu\frac{\partial v_z}{\partial r} - \rho\overline{v_z' v_r'} \tag{3}$$

$$\dot{q}_r = -k\frac{\partial T}{\partial r} + \rho c_p \overline{v_r' T'}. \tag{4}$$

According to experiments by Kikuyama et al. [4], the

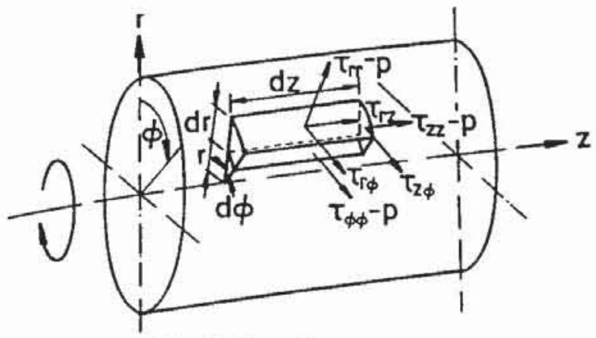

FIG. 1. Coordinate system.

distribution of the tangential velocity can be assumed to be that of solid body rotation

$$v_\phi = \frac{r}{R} v_{\phi w}. \tag{5}$$

After some manipulations and after introduction of the turbulence model, as described in ref. [9], the axial momentum equation and the energy equation can be written in the following dimensionless form:

axial momentum equation

$$\left(\frac{l}{R}\right)^2 \left(\frac{d\tilde{v}_z}{d\tilde{r}}\right)^2 - \frac{1}{Re_*}\frac{d\tilde{v}_z}{d\tilde{r}} - \tilde{r} = 0; \tag{6}$$

energy equation

$$\tilde{v}_z \frac{\partial \theta}{\partial \tilde{z}} = \frac{1}{\tilde{r}}\frac{\partial}{\partial \tilde{r}}\left(\left[1 - Pr\, Re_* \frac{l}{R}\frac{l_q}{R}\left(\frac{\partial \tilde{v}_z}{\partial \tilde{r}}\right)\right]\tilde{r}\frac{\partial \theta}{\partial \tilde{r}}\right). \tag{7}$$

Here $\tilde{r} = r/R$ is the dimensionless radius. Furthermore, the following dimensionless quantities are introduced in equations (6) and (7):

$$Re = \frac{\bar{v}_z D}{\nu} \tag{8}$$

$$Re_* = \frac{v_* R}{\nu} \tag{9}$$

$$Re_\phi = \frac{v_{\phi w} D}{\nu} \tag{10}$$

$$N = \frac{v_{\phi w}}{\bar{v}_z} = \frac{Re_\phi}{Re} \tag{11}$$

$$\tilde{z} = \frac{zk}{\rho c_p v_* R^2} = \frac{z}{R}\frac{1}{Re_* Pr} \tag{12}$$

$$\theta = \frac{T - T_0}{\dfrac{\mathring{q}_{rw} R}{k}}. \tag{13}$$

The hydrodynamic mixing length l and the thermal mixing length l_q in the rotating pipe are obtained from the mixing length in a stationary pipe, i.e. from the modified Nikuradse mixing length expression

$$\frac{l_0}{R} = [1 - e^{-y^+/26}]\left[0.14 - 0.08\left(\frac{r}{R}\right)^2 - 0.06\left(\frac{r}{R}\right)^4\right] \tag{14}$$

the reciprocal of the turbulent Prandtl number

$$\frac{1}{Pr_t} = \frac{l_{q0}}{l_0} = 1.53 - 2.82\tilde{r}^2 + 3.85\tilde{r}^3 - 1.48\tilde{r}^4 \tag{15}$$

and a semi-empirical expression for the ratio of the mixing lengths in a rotating and a stationary pipe, which was found in ref. [5]

$$\frac{l}{l_0} = \frac{l_q}{l_{q0}} = 0.4\sqrt{N}. \tag{16}$$

Further solution of the conservation equations is performed in analogy to ref. [9] and will not be described again.

2.2. *Results and discussion*

The effects of rotation on the axial and tangential velocity distribution for fully developed flow conditions are shown in Figs. 2 and 3 for different flow-rate Reynolds numbers. Experimental results of Kikuyama *et al.* [4] have been plotted for comparison. The validity of the assumption of a linear tangential velocity profile is well confirmed by the experiments. The calculated profiles of the axial velocity are in good agreement with the experiments. The shape of the axial velocity profile is largely independent of the flow-rate Reynolds number. With increasing rotational Reynolds number Re_ϕ the parabolic axial velocity profile of the Hagen–Poiseuille flow shifts towards that of turbulent pipe flow.

In Fig. 4 the friction factor λ is plotted vs the flow-rate Reynolds number Re for various values of the rotational Reynolds number Re_ϕ. Without rotation, $Re_\phi = 0$, the friction law of the Hagen–Poiseuille flow, $\lambda = 64/Re$, is valid. With growing rotational speed an increase in λ can be observed.

The influence of rotation on the temperature distribution for fully developed hydrodynamic and thermal boundary layers is depicted in Fig. 5. With an increasing rotational Reynolds number the laminar temperature profiles approach that for turbulent pipe flow. Unfortunately there are no experimental temperature profiles available.

In Fig. 6 the Nusselt number is plotted as a function of the flow-rate Reynolds number Re with the rotational Reynolds number Re_ϕ as a parameter. For $Re_\phi = 0$, i.e. for laminar pipe flow without rotation, the Nusselt number has the constant value $Nu = 4.36$. With growing rotational Reynolds number Re_ϕ the Nusselt number increases. In contrast to the constant Nusselt number in the case of no rotation, the Nusselt number increases slightly with a growing Reynolds number, if $Re_\phi > 0$.

3. INTERACTION OF ROTATION AND THERMAL BUOYANCY FORCES

Utilizing the profiles of the axial velocity and the temperature calculated above, a perturbation cal-

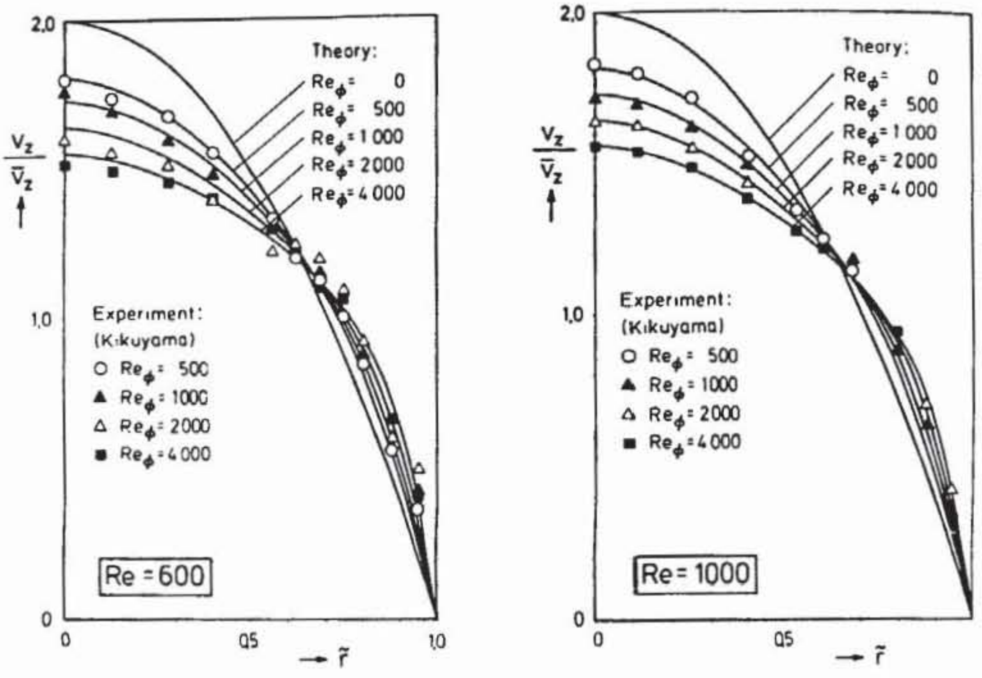

FIG. 2. Axial velocity distribution as a function of the rotational Reynolds number Re_ϕ.

culation will be performed, which will describe the formation of a secondary flow due to buoyancy forces and its decay owing to centrifugal forces in the case of pipe rotation.

3.1. *Mathematical formulation*

Denoting the coordinate system, as illustrated in Fig. 1, by $\tilde{r}$, ϕ, $\tilde{z}$ as dimensionless radial, tangential and axial coordinates, with the corresponding dimensionless velocities $\tilde{v}_r^*$, $\tilde{v}_\phi^*$, $\tilde{v}_z^*$ and the dimensionless temperature $\tilde{\theta}^*$, the equations of conservation for a fully developed flow of an incompressible, newtonian fluid in a horizontal pipe, in consideration of gravitational forces, take the following form:

continuity equation

$$\frac{\partial(\tilde{v}_r^*\tilde{r})}{\partial\tilde{r}} + \frac{\partial\tilde{v}_\phi^*}{\partial\phi} = 0; \tag{17}$$

radial momentum equation

$$\tilde{v}_r^*\frac{\partial\tilde{v}_r^*}{\partial\tilde{r}} + \frac{\tilde{v}_\phi^*}{\tilde{r}}\frac{\partial\tilde{v}_r^*}{\partial\phi} - \frac{\tilde{v}_\phi^{*2}}{\tilde{r}} = -\frac{\partial\tilde{p}^*}{\partial\tilde{r}} + \frac{2}{Re}\left(\nabla^2\tilde{v}_r^* - \frac{\tilde{v}_r^*}{\tilde{r}^2} - \frac{2}{\tilde{r}^2}\frac{\partial\tilde{v}_\phi^*}{\partial\phi}\right) - \frac{1}{2}\frac{Gr}{Re^2}\cos\phi(1-\tilde{\theta}^*); \tag{18}$$

tangential momentum equation

$$\tilde{v}_r^*\frac{\partial\tilde{v}_\phi^*}{\partial\tilde{r}} + \frac{\tilde{v}_\phi^*}{\tilde{r}}\frac{\partial\tilde{v}_\phi^*}{\partial\phi} + \frac{\tilde{v}_r^*\tilde{v}_\phi^*}{\tilde{r}} = -\frac{1}{\tilde{r}}\frac{\partial\tilde{p}^*}{\partial\phi} + \frac{2}{Re}\left(\nabla^2\tilde{v}_\phi^* + \frac{2}{\tilde{r}^2}\frac{\partial\tilde{v}_r^*}{\partial\phi} - \frac{\tilde{v}_\phi^*}{\tilde{r}^2}\right) + \frac{1}{2}\frac{Gr}{Re^2}\sin\phi(1-\tilde{\theta}^*); \tag{19}$$

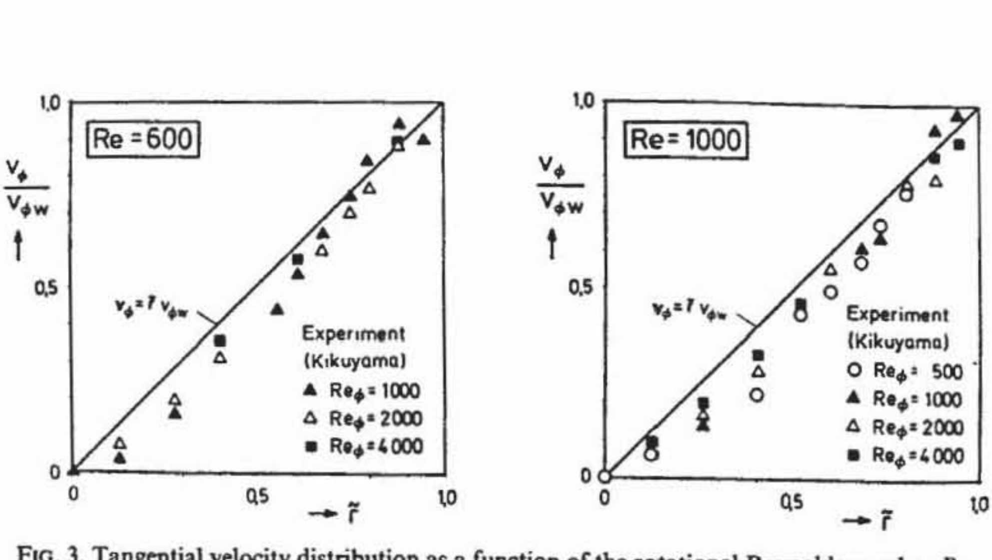

FIG. 3. Tangential velocity distribution as a function of the rotational Reynolds number Re_ϕ.

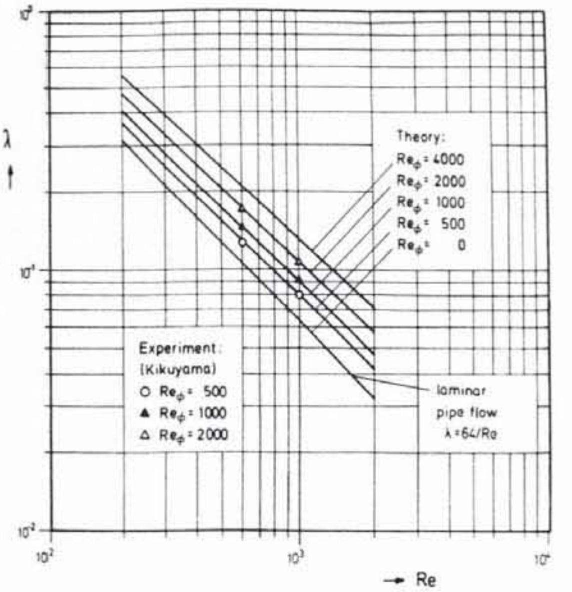

FIG. 4. Friction coefficient λ of the rotating pipe as a function of Re with Re_ϕ as a parameter.

axial momentum equation

$$\tilde{v}_r^* \frac{\partial \tilde{v}_z^*}{\partial \tilde{r}} + \frac{\tilde{v}_\phi^*}{\tilde{r}} \frac{\partial \tilde{v}_z^*}{\partial \phi} = -\frac{\partial \tilde{p}^*}{\partial \tilde{z}} + \frac{2}{Re} \nabla^2 \tilde{v}_z^*; \quad (20)$$

energy equation

$$\tilde{v}_r^* \frac{\partial \tilde{\theta}^*}{\partial \tilde{r}} + \frac{\tilde{v}_\phi^*}{\tilde{r}} \frac{\partial \tilde{\theta}^*}{\partial \phi} + \tilde{v}_z^* C_0 = \frac{2}{Re\,Pr} \nabla^2 \tilde{\theta}^* \quad (21)$$

with the dimensionless quantities

$$\tilde{r} = \frac{r}{R}; \quad \tilde{v}_i^* = \frac{v_i}{\bar{v}_z}; \quad i = r, \phi, z$$

$$\tilde{\theta}^* = \frac{T - T_0}{T_w - T_0}; \quad \tilde{p}^* = \frac{p}{\rho \bar{v}_z^2}$$

$$Pr = \frac{v}{a}$$

$$Re = \frac{\bar{v}_z D}{v}$$

$$Gr = \beta g \frac{(T_w - T_0) D^3}{v^2} = \frac{\beta g \Delta T D^3}{v^2}$$

$$C_0 = \frac{4\mathring{q}_{r,w} R}{k \Delta T} \frac{1}{Re\,Pr} \quad (22)$$

and the Laplacian operator

$$\nabla^2 \equiv \frac{\partial^2}{\partial \tilde{r}^2} + \frac{1}{\tilde{r}} \frac{\partial}{\partial \tilde{r}} + \frac{1}{\tilde{r}^2} \frac{\partial^2}{\partial \phi^2}. \quad (23)$$

Provided that the buoyancy terms in equations (18) and (19) are small as compared to unity, successive approximations to the solution can be determined by expanding $\tilde{v}_i^*$, $\tilde{p}^*$ and $\tilde{\theta}^*$ as power series in $\varepsilon = Gr/Re^2$

$$\begin{aligned} \tilde{v}_i^* &= \tilde{v}_{i0} + \varepsilon \tilde{v}_{i1} + \varepsilon^2 \tilde{v}_{i2} + \tilde{v}_i', \quad i = r, \phi, z \\ \tilde{p}^* &= \tilde{p}_0 + \varepsilon \tilde{p}_1 + \varepsilon^2 \tilde{p}_2 + \tilde{p}' \\ \tilde{\theta}^* &= \tilde{\theta}_0 + \varepsilon \tilde{\theta}_1 + \varepsilon^2 \tilde{\theta}_2 + \tilde{\theta}'. \end{aligned} \quad (24)$$

The turbulent values, $\tilde{v}_i'$, $\tilde{p}'$, $\tilde{\theta}'$ will not be effected by the secondary motion, if $\varepsilon \ll 1$, as shown by Polyakov [10]. Hence these values are not expanded as power series in equation (24).

Introducing equation (24) into equations (17)–(21)

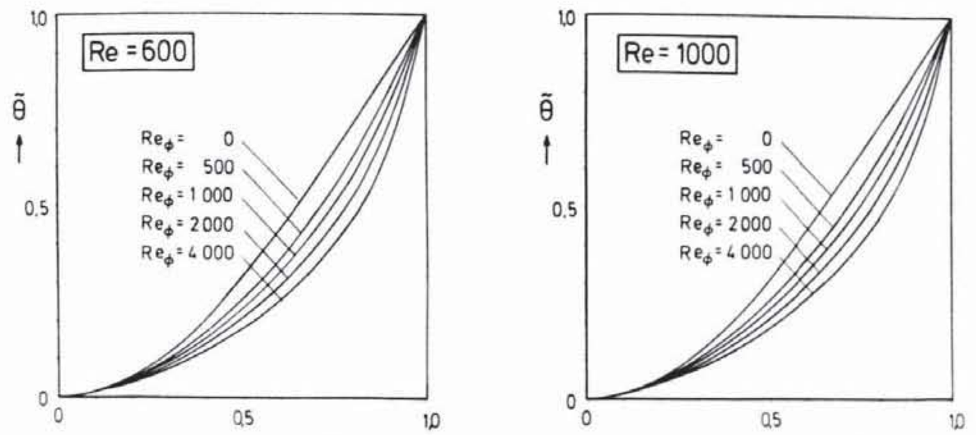

FIG. 5. Temperature distribution as a function of the rotational Reynolds number Re_ϕ [$\tilde{\theta} = (T(\tilde{r}) - T(\tilde{r} = 0))/(T(\tilde{r} = 1) - T(\tilde{r} = 0))$].

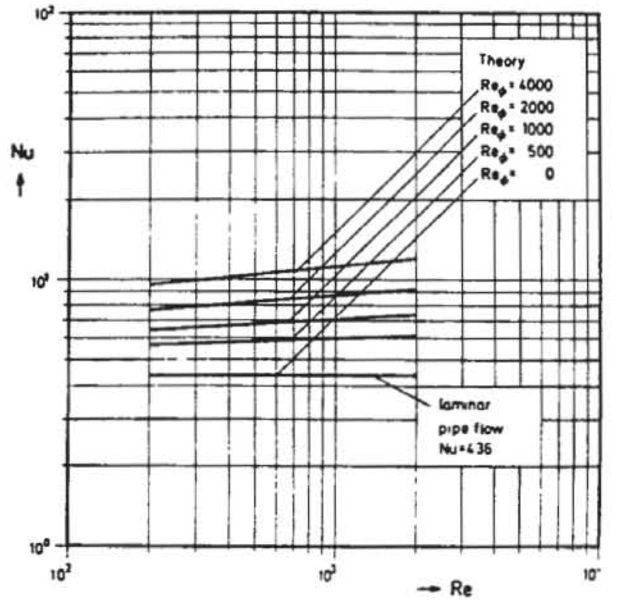

FIG. 6. Nusselt number Nu of the rotating pipe as a function of Re with Re_ϕ as a parameter.

and neglecting terms in ε and ε^2, yields the zeroth-order equations for the flow in a rotating tube without free convection, which have been solved in Section 2.

The elimination of the pressure in equations (18) and (19) and the introduction of the stream function

$$\tilde{v}_r\tilde{r} = \frac{\partial\psi}{\partial\phi}, \quad \tilde{v}_\phi = -\frac{\partial\psi}{\partial\tilde{r}} \tag{25}$$

results in first-order equations for ψ, $\tilde{v}_z$ and $\tilde{\theta}$, if terms of the order of ε^2 are neglected

$$\frac{2}{Re}\nabla^4\psi_1 + \frac{1}{\tilde{r}}\left(\frac{\partial\psi_0}{\partial\tilde{r}}\frac{\partial}{\partial\phi}\nabla^2\psi_1\right) = -\frac{1}{2}\frac{\partial\tilde{\theta}_0}{\partial\tilde{r}}\sin\phi \tag{26}$$

$$\frac{2}{Re}\nabla^2\tilde{v}_{z1} + \frac{1}{\tilde{r}}\left(\frac{\partial\psi_0}{\partial\tilde{r}}\frac{\partial\tilde{v}_{z1}}{\partial\phi}\right) = \frac{1}{\tilde{r}}\frac{\partial\psi_1}{\partial\phi}\frac{\partial\tilde{v}_{z0}}{\partial\tilde{r}} \tag{27}$$

$$\frac{2}{Re\,Pr}\nabla^4\tilde{\theta}_1 + \frac{1}{\tilde{r}}\left(\frac{\partial\psi_0}{\partial\tilde{r}}\frac{\partial\tilde{\theta}_1}{\partial\phi}\right) = \frac{1}{\tilde{r}}\frac{\partial\psi_1}{\partial\phi}\frac{\partial\tilde{\theta}_0}{\partial\tilde{r}} + C_0\tilde{v}_{z1} \tag{28}$$

and in second-order equations

$$\frac{2}{Re}\nabla^4\psi_2 + \frac{1}{\tilde{r}}\left(\frac{\partial\psi_0}{\partial\tilde{r}}\frac{\partial}{\partial\phi}\nabla^2\psi_2\right) = -\frac{1}{2}\left(\frac{\partial\tilde{\theta}_1}{\partial\tilde{r}}\sin\phi + \frac{\partial\tilde{\theta}_1}{\partial\phi}\cos\phi\right) + \frac{2}{\tilde{r}}\frac{\partial\psi_1}{\partial\phi}\frac{\partial\nabla^2\psi_1}{\partial\tilde{r}} - \frac{1}{\tilde{r}}\frac{\partial\psi_1}{\partial\tilde{r}}\frac{\partial\nabla^2\psi_1}{\partial\phi} \tag{29}$$

$$\frac{2}{Re}\nabla^2\tilde{v}_{z2} + \frac{1}{\tilde{r}}\left(\frac{\partial\psi_0}{\partial\tilde{r}}\frac{\partial\tilde{v}_{z2}}{\partial\phi}\right) = \frac{1}{\tilde{r}}\left(-\frac{\partial\psi_1}{\partial\tilde{r}}\frac{\partial\tilde{v}_{z1}}{\partial\phi} + \frac{\partial\psi_2}{\partial\phi}\frac{\partial\tilde{v}_{z0}}{\partial\tilde{r}} + \frac{\partial\psi_1}{\partial\phi}\frac{\partial\tilde{v}_{z1}}{\partial\tilde{r}}\right) \tag{30}$$

$$\frac{2}{Re\,Pr}\nabla^2\tilde{\theta}_2 + \frac{1}{\tilde{r}}\left(\frac{\partial\psi_0}{\partial\tilde{r}}\frac{\partial\tilde{\theta}_2}{\partial\phi}\right) = C_0\tilde{v}_{z2} - \frac{1}{\tilde{r}}\left(\frac{\partial\psi_1}{\partial\tilde{r}}\frac{\partial\tilde{\theta}_1}{\partial\phi} - \frac{\partial\psi_2}{\partial\phi}\frac{\partial\tilde{\theta}_0}{\partial\tilde{r}} - \frac{\partial\psi_1}{\partial\phi}\frac{\partial\tilde{\theta}_1}{\partial\tilde{r}}\right) \tag{31}$$

with the boundary conditions

$$\frac{1}{\tilde{r}}\frac{\partial\psi_{1,2}}{\partial\phi}\bigg|_{\tilde{r}=1} = -\frac{\partial\psi_{1,2}}{\partial\tilde{r}}\bigg|_{\tilde{r}=1} = 0$$

$$\frac{1}{\tilde{r}}\frac{\partial\psi_{1,2}}{\partial\phi}\bigg|_{\tilde{r}=0} = \text{finite}, \quad -\frac{\partial\psi_{1,2}}{\partial\tilde{r}}\bigg|_{\tilde{r}=0} = \text{finite}$$

$$\tilde{v}_{z1,2}(\tilde{r}=0,\phi) = \text{finite}$$

$$\tilde{v}_{z1,2}(\tilde{r}=1,\phi) = 0$$

$$\tilde{\theta}_{1,2}(\tilde{r}=0,\phi) = \text{finite}$$

$$\tilde{\theta}_{1,2}(\tilde{r}=1,\phi) = 0. \tag{32}$$

According to experiments by Kikuyama et al. [4], the stream function in the case of no rotation, ψ_0, is defined by

$$\psi_0 = -\frac{1}{2}\frac{Re_\phi}{Re}\tilde{r}^2. \tag{33}$$

With this expression equations (26)–(31) can be written in the following form:

$$\nabla^4\psi_1 - \frac{Re_\phi}{2}\frac{\partial}{\partial\phi}\nabla^2\psi_1 = -\frac{Re}{4}\frac{\partial\tilde{\theta}_0}{\partial\tilde{r}}\sin\phi \tag{34}$$

$$\nabla^2\tilde{v}_{z1} - \frac{Re_\phi}{2}\frac{\partial\tilde{v}_{z1}}{\partial\phi} = \frac{Re}{2}\frac{1}{\tilde{r}}\frac{\partial\psi_1}{\partial\phi}\frac{\partial\tilde{v}_{z0}}{\partial\tilde{r}} \tag{35}$$

$$\frac{1}{Pr}\nabla^2\tilde{\theta}_1 - \frac{Re_\phi}{2}\frac{\partial\tilde{\theta}_1}{\partial\phi} = \frac{Re}{2}\left(\frac{1}{\tilde{r}}\frac{\partial\psi_1}{\partial\phi}\frac{\partial\tilde{\theta}_0}{\partial\tilde{r}} + C_0\tilde{v}_{z1}\right) \tag{36}$$

$$\nabla^4\psi_2 - \frac{Re_\phi}{2}\frac{\partial}{\partial\phi}\nabla^2\psi_2 = -\frac{Re}{4}\left(\frac{\partial\tilde{\theta}_1}{\partial\tilde{r}}\sin\phi + \frac{\partial\tilde{\theta}_1}{\partial\phi}\cos\phi\right) + \frac{Re}{2}\frac{1}{\tilde{r}}\left(\frac{\partial\psi_1}{\partial\phi}\frac{\partial\nabla^2\psi_1}{\partial\tilde{r}} - \frac{\partial\psi_1}{\partial\tilde{r}}\frac{\partial\nabla^2\psi_1}{\partial\phi}\right) \tag{37}$$

$$\nabla^2\tilde{v}_{z2} - \frac{Re_\phi}{2}\frac{\partial\tilde{v}_{z2}}{\partial\phi} = -\frac{Re}{2}\frac{1}{\tilde{r}}\left(\frac{\partial\psi_1}{\partial\tilde{r}}\frac{\partial\tilde{v}_{z1}}{\partial\phi} - \frac{\partial\psi_2}{\partial\phi}\frac{\partial\tilde{v}_{z0}}{\partial\tilde{r}} - \frac{\partial\psi_1}{\partial\phi}\frac{\partial\tilde{v}_{z1}}{\partial\tilde{r}}\right) \tag{38}$$

$$\frac{1}{Pr}\nabla^2\tilde{\theta}_2 - \frac{Re_\phi}{2}\frac{\partial\tilde{\theta}_2}{\partial\phi} = \frac{Re}{2}\left(C_0\tilde{v}_{z2} - \frac{1}{\tilde{r}}\left(\frac{\partial\psi_1}{\partial\tilde{r}}\frac{\partial\tilde{\theta}_1}{\partial\phi} - \frac{\partial\psi_2}{\partial\phi}\frac{\partial\tilde{\theta}_0}{\partial\tilde{r}} - \frac{\partial\psi_1}{\partial\phi}\frac{\partial\tilde{\theta}_1}{\partial\tilde{r}}\right)\right). \tag{39}$$

Without free convection effects, profiles of the axial velocity $\tilde{v}_{z0}(\tilde{r})$ and of the temperature $\tilde{\theta}_0(\tilde{r})$ have been calculated in Section 2. Since they are the results of a numerical calculation, they will be approximated by the following polynomial expressions:

$$\tilde{\theta}_0 = m_0 + m_1\tilde{r}^2 + m_2\tilde{r}^4 \tag{40}$$

$$\tilde{v}_{z0} = n_0 + n_1\tilde{r}^2 + n_2\tilde{r}^4. \tag{41}$$

The maximum deviation of equations (40) and (41) from the numerical results is less than 3%, which is a sufficient accuracy for the following considerations.

Substituting the stream function in equation (34) by

$$\psi_1 = f_1(\tilde{r})\sin\phi + f_2(\tilde{r})\cos\phi \tag{42}$$

yields two coupled ordinary differential equations

$$f_1'''' + \frac{2}{\tilde{r}}f_1''' - \frac{3}{\tilde{r}^2}f_1'' + \frac{3}{\tilde{r}^3}f_1' - \frac{3}{\tilde{r}^4}f_1 + \frac{Re_\phi}{2}\left(f_2'' + \frac{1}{\tilde{r}}f_2' - \frac{1}{\tilde{r}^2}f_2\right) = -\frac{Re}{4}\frac{\partial\tilde{\theta}_0}{\partial\tilde{r}} \tag{43}$$

$$f_2'''' + \frac{2}{\tilde{r}}f_2''' - \frac{3}{\tilde{r}^2}f_2'' + \frac{3}{\tilde{r}^3}f_2' - \frac{3}{\tilde{r}^4}f_2 - \frac{Re_\phi}{2}\left(f_1'' + \frac{1}{\tilde{r}}f_1' - \frac{1}{\tilde{r}^2}f_1\right) = 0 \tag{44}$$

with the boundary conditions

$$\begin{aligned} &f_1(1) = 0, \quad f_1(0) = \text{finite} \\ &f_1'(1) = 0, \quad f_1'(0) = \text{finite} \\ &f_2(1) = 0, \quad f_2(0) = \text{finite} \\ &f_2'(1) = 0, \quad f_2'(0) = \text{finite}. \end{aligned} \tag{45}$$

Introducing the complex function

$$V = f_1 + \mathrm{i}f_2 \tag{46}$$

into equations (43) and (44) and summing up both equations results in the following complex ordinary differential equation of the fourth order:

$$V'''' + \frac{2}{\tilde{r}}V''' - \frac{3}{\tilde{r}^2}V'' + \frac{3}{\tilde{r}^3}V' - \frac{3}{\tilde{r}^4}V + \frac{Re_\phi}{2\mathrm{i}}\left(V'' + \frac{1}{\tilde{r}}V' - \frac{1}{\tilde{r}^2}V\right) = -\frac{Re}{4}\frac{\partial\tilde{\theta}_0}{\partial\tilde{r}} \tag{47}$$

with the boundary conditions

$$\begin{aligned} &V(1) = 0, \quad V(0) = \text{finite} \\ &V'(1) = 0, \quad V'(0) = \text{finite}. \end{aligned} \tag{48}$$

Equation (47) can be reduced to an ordinary differential equation of the second order by introducing the following function:

$$U = V'' + \frac{1}{\tilde{r}}V' - \frac{1}{\tilde{r}^2}V = \frac{\mathrm{d}}{\mathrm{d}r}\left[\frac{1}{r}\frac{\mathrm{d}}{\mathrm{d}r}(rV)\right]. \tag{49}$$

From equation (49) V can be determined as

$$V = \frac{1}{\tilde{r}}\int(\textstyle\int U\,\mathrm{d}\tilde{r})\tilde{r}\,\mathrm{d}\tilde{r} + C_1\tilde{r} + \frac{C_2}{\tilde{r}}. \tag{50}$$

By use of equation (49) and with the polynomial expression for the temperature (equation (40)), the differential equation (47) can be written as

$$\tilde{r}^2U''(\tilde{r}) + \tilde{r}U'(\tilde{r}) + \left(\frac{Re_\phi}{2\mathrm{i}}\tilde{r}^2 - 1\right)U(\tilde{r}) = -\frac{1}{2}Re\,m_1\tilde{r}^3 - Re\,m_2\tilde{r}^5. \tag{51}$$

Introducing the coordinate transformation

$$\delta = \sqrt{\left(\frac{Re_\phi}{2\mathrm{i}}\right)}\tilde{r} \tag{52}$$

into equation (51) yields a Bessel differential equation

$$\delta^2U''(\delta) + \delta U'(\delta) + (\delta^2 - 1)U(\delta) = -\frac{1}{2}Re\,m_1\left(\frac{2\mathrm{i}}{Re_\phi}\right)^{3/2}\delta^3 - Re\,m_2\left(\frac{2\mathrm{i}}{Re_\phi}\right)^{5/2}\delta^5 \tag{53}$$

which has the solution

$$U(\delta) = C_3J_1(\delta) + C_4Y_1(\delta) + \left[-\frac{1}{2}Re\,m_1\left(\frac{2\mathrm{i}}{Re_\phi}\right)^{3/2} + 8Re\,m_2\left(\frac{2\mathrm{i}}{Re_\phi}\right)^{5/2}\right]\delta - Re\,m_2\left(\frac{2\mathrm{i}}{Re_\phi}\right)^{5/2}\delta^3 \tag{54}$$

J_1 is the Bessel function of the first order

$$J_1(\delta) = \sum_{\nu=0}^{\infty}\frac{(-1)^\nu}{\nu!(\nu+1)!}\left(\frac{\delta}{2}\right)^{2\nu+1} \tag{55}$$

Y_1 is the Weber function of the first order

$$Y_1(\delta) = \frac{2}{\pi}\left[E + \ln\left(\frac{\delta}{2}\right)\right]J_1(\delta) - \frac{2}{\pi}\frac{1}{\delta} - \frac{1}{\pi}\sum_{\nu=0}^{\infty}\frac{(-1)^\nu}{\nu!(\nu+1)!}\left(\frac{\delta}{2}\right)^{2\nu+1}\left(\sum_{s=1}^{\nu+1}\frac{1}{s} + \sum_{s=1}^{\nu}\frac{1}{s}\right)$$

$(E = 0.5772$ is the Eulerian constant) (56)

C_3 and C_4 are constants which must be determined. $V(\delta)$ is calculated by the inverse transformation (equation (50))

$$V(\delta) = \frac{2\mathrm{i}}{Re_\phi}\frac{1}{\delta}\int(\delta\textstyle\int U(\delta)\,\mathrm{d}\delta)\,\mathrm{d}\delta + C_5\delta + C_6\frac{1}{\delta} \tag{57}$$

$$V(\delta) = D_1J_1(\delta) + D_2Y_1(\delta) + D_3\frac{1}{\delta} + D_4\delta + D_5\delta^3 + D_6\delta^5. \tag{58}$$

The constants D_i are given in the Appendix. An adaption of the solution $V(\delta)$ to the boundary conditions (equation (48)) results in

$$V(\delta) = D_1J_1(\delta) + D_4\delta + D_5\delta^3 + D_6\delta^5. \tag{59}$$

Splitting of the complex function $V(\delta)$ into the real part and the imaginary part yields the functions f_1 and f_2, and the stream function $\psi_1(\tilde{r}, \phi)$ can be determined as

$$\psi_1(\tilde{r}, \phi) = \left[d_{1R} \sum_{v=0}^{\infty} K_v \tilde{r}^{4v+1} - d_{1I} \sum_{v=0}^{\infty} L_v \tilde{r}^{4v+3} + d_{4R}\tilde{r} + d_{5R}\tilde{r}^3 \right] \sin\phi + \left[d_{1I} \sum_{v=0}^{\infty} K_v \tilde{r}^{4v+1} + d_{1R} \sum_{v=0}^{\infty} L_v \tilde{r}^{4v+3} + d_{4I}\tilde{r} + d_{5I}\tilde{r}^3 + d_{6I}\tilde{r}^5 \right] \cos\phi \quad (60)$$

where the constants d_{iR}, d_{iI}, K_v and L_v are given in the Appendix.

For $Re_\phi \to 0$, which corresponds to the flow in a non-rotating pipe, the function $f_2(\tilde{r})$ approaches linearly with Re_ϕ the value zero. The function $f_1(\tilde{r})$ approaches the solution of Morton [6]

$$\lim_{Re_\phi \to 0} \psi_1(\tilde{r}, \phi) = -\frac{Re\, m_2}{1152} \left(\tilde{r}^6 + 3\frac{m_1}{m_2}\tilde{r}^4 - 3\left(2\frac{m_1}{m_2} + 1\right)\tilde{r}^2 + \left(3\frac{m_1}{m_2} + 2\right)\right) \tilde{r} \sin\phi. \quad (61)$$

The corresponding temperature distribution is that of the laminar Hagen–Poiseuille flow, with $m_1 = 4/3$ and $m_2 = -1/3$.

The axial velocity distribution is calculated with the same procedure as the stream function ψ_1. By use of equation (41) and with the statement

$$\tilde{v}_{z1} = f_3(\tilde{r})\sin\phi + f_4(\tilde{r})\cos\phi \quad (62)$$

equation (35) can be transformed into two coupled ordinary differential equations

$$f_3'' + \frac{1}{\tilde{r}} f_3' - \frac{1}{\tilde{r}^2} f_3 + \frac{Re_\phi}{2} f_4 = -Re(n_1 + 2n_2\tilde{r}^2) f_2 \quad (63)$$

$$f_4'' + \frac{1}{\tilde{r}} f_4' - \frac{1}{\tilde{r}^2} f_4 - \frac{Re_\phi}{2} f_3 = -Re(n_1 + 2n_2\tilde{r}^2) f_1 \quad (64a)$$

with the boundary conditions

$$f_3(0) = f_4(0) = \text{finite}$$
$$f_3(1) = f_4(1) = 0. \quad (64b)$$

Introduction of the complex function

$$W(\tilde{r}) = f_3 + \mathrm{i} f_4 \quad (65)$$

and transformation of the coordinate $\tilde{r}$ to δ results in the following non-homogeneous Bessel differential equation:

$$\delta^2 W''(\delta) + \delta W'(\delta) + (\delta^2 - 1) W(\delta) = (B_1\delta^2 + B_2\delta^4) J_1(\delta) + B_3\delta^3 + B_4\delta^5 + B_5\delta^7 + B_6\delta^9 \quad (66a)$$

with the boundary conditions

$$W(0) = \text{finite}$$
$$W\left(\sqrt{\left(\frac{Re_\phi}{2\mathrm{i}}\right)}\right) = 0 \quad (66b)$$

and the constants B_i given in the Appendix. The solution of the differential equation (66a), which satisfies the accompanying boundary conditions, is

$$W(\delta) = E_1 J_1(\delta) + E_3\delta^2 J_1(\delta) + (E_4\delta + E_5\delta^3) J_0(\delta) + E_6\delta + E_7\delta^3 + E_8\delta^5 + E_9\delta^7. \quad (67)$$

The constants E_i are given in the Appendix, too.

By splitting this solution into the real part and the imaginary part, we get the perturbation velocity $\tilde{v}_{z1}$

$$\tilde{v}_{z1}(\tilde{r}, \phi) = \left[(e_{1R} + e_{3R}\tilde{r}^2) \sum_{v=0}^{\infty} K_v \tilde{r}^{4v+1} - (e_{1I} + e_{3I}\tilde{r}^2) \sum_{v=0}^{\infty} L_v \tilde{r}^{4v+3} + (e_{4R} + e_{5R}\tilde{r}^2) \times \sum_{v=0}^{\infty} K_v(4v+2)\tilde{r}^{4v+1} + e_{6R}\tilde{r} + e_{7R}\tilde{r}^3 - (e_{4I} + e_{5I}\tilde{r}^2) \times \sum_{v=0}^{\infty} L_v(4v+4)\tilde{r}^{4v+3} + e_{8R}\tilde{r}^5 \right] \sin\phi + \left[(e_{1I} + e_{3I}\tilde{r}^2) \sum_{v=0}^{\infty} K_v \tilde{r}^{4v+1} + (e_{1R} + e_{3R}\tilde{r}^2) \times \sum_{v=0}^{\infty} L_v \tilde{r}^{4v+3} + (e_{4I} + e_{5I}\tilde{r}^2) \sum_{v=0}^{\infty} K_v(4v+2)\tilde{r}^{4v+1} + e_{6I}\tilde{r} + e_{7I}\tilde{r}^3 + (e_{4R} + e_{5R}\tilde{r}^2) \sum_{v=0}^{\infty} L_v(4v+4)\tilde{r}^{4v+3} + e_{8I}\tilde{r}^5 + e_{9I}\tilde{r}^7 \right] \cos\phi. \quad (68)$$

The constants e_{iI} and e_{iR} are listed in the Appendix. The time-smoothed axial velocity $\tilde{v}_z$ is given by

$$\tilde{v}_z = \tilde{v}_{z0} + \varepsilon \tilde{v}_{z1} = \tilde{v}_{z0} + \frac{Gr}{Re^2}\tilde{v}_{z1}. \quad (69)$$

After some manipulations it can be demonstrated, that this solution for $Re_\phi \to 0$ approaches that of Morton [6] for the fluid flow in a non-rotating pipe ($n_1 = -2$, $n_2 = 0$)

$$\lim_{Re_\phi \to 0} \tilde{v}_{z1} = -\frac{Re^2}{138\,240}(1 - \tilde{r}^2) \times (49 - 51\tilde{r}^2 + 19\tilde{r}^4 - \tilde{r}^6)\tilde{r}\cos\phi. \quad (70)$$

The temperature distribution $\tilde{\theta}_1$ can be obtained by the same procedure as for the stream function and the axial velocity. However, the expressions for $\tilde{\theta}$ are very lengthy and monstrous. Therefore, they are omitted in this paper.

The following conclusions may be drawn by a detailed consideration of the differential equations (34)–(39).

(1) In the case of no rotation, for $Re_\phi \to 0$, the perturbations ψ_1, $\tilde{v}_{z1}$, $\tilde{\theta}_1$, ψ_2, $\tilde{v}_{z2}$, $\tilde{\theta}_2$ attain their maximum values, which corresponds to Morton's [6] solution.

(2) It can be seen that ψ_1 approaches linearly the limiting value zero for $Re_\phi \to \infty$. $\tilde{v}_{z1}$ approaches zero quadratically with increasing Re_ϕ.

(3) ψ_2 approaches zero with Re_ϕ^4, $\tilde{v}_{z2}$ and $\tilde{\theta}_2$ approach zero with Re_ϕ^4.

Since the perturbations of the second order may be neglected already in the case of no rotation [6], they may be disregarded for $Re_\phi > 0$, too. For small values of Re_ϕ ($Re_\phi \leqslant 200$) Morton's solution for the temperature distribution [6] may be used as an approximation for $\tilde{\theta}$. For an increasing rotational speed ($Re_\phi > 200$) the free convection effects on the temperature distribution may be neglected, since $\tilde{\theta}_1$ approaches zero with Re_ϕ^2.

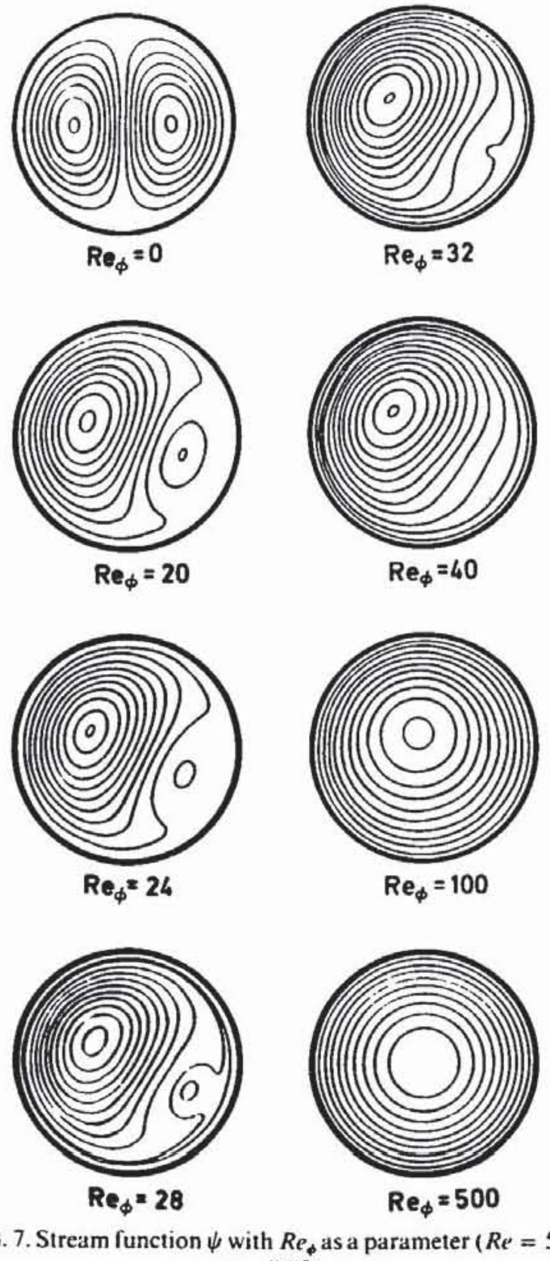

FIG. 7. Stream function ψ with Re_ϕ as a parameter ($Re = 500$, $\varepsilon = 0.05$).

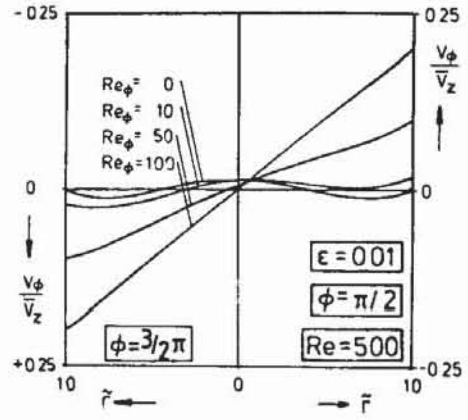

FIG. 8. Tangential velocity as a function of the rotational Reynolds number Re_ϕ.

3.2. *Results and discussion*

Figure 7 shows the effect of rotation on the free convection flow. To demonstrate this effect, streamlines are plotted for constant Re and ε ($Re = 500$; $\varepsilon = 0.05$) and for different rotational Reynolds numbers, $0 \leqslant Re_\phi \leqslant 500$. Already small temperature differences between the heated wall and the fluid cause a secondary flow. There exist two counterrotating convection cells, flowing upward at the pipe wall and downward in the pipe centre. If this convection flow is superposed by a clockwise rotation of the tube, the corotating left-hand convection cell grows, while the counterrotating cell vanishes with growing Re_ϕ. This effect of the growing corotating and the diminishing counterrotating convection cell is evident in the range $20 \leqslant Re_\phi \leqslant 40$. For $Re_\phi \geqslant 40$ the right-hand cell has disappeared and the left-hand cell covers the whole cross-section. The 'eye' of the convection cell, however, is located above the pipe centre. With increasing Re_ϕ the eccentricity of the cell diminishes and for $Re_\phi \geqslant 500$ a rigid body rotation is established.

The effects of the interaction of free convection and rotation are shown in Figs. 8 and 9. In Fig. 8 profiles of the tangential velocity in a horizontal sectional plane are plotted with Re_ϕ as a parameter. Without rotation, for $Re_\phi = 0$, there is an upward flow near the pipe wall and a downward flow near the pipe axis. With increasing rotational speed the rotation-induced

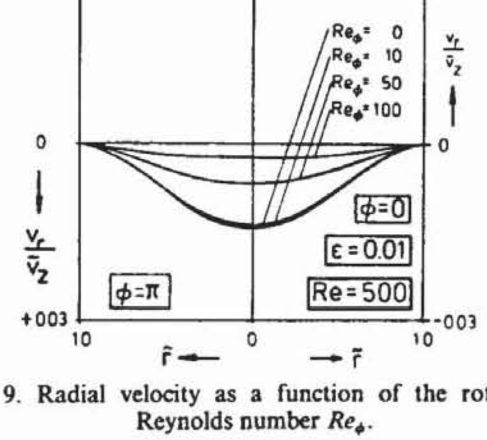

FIG. 9. Radial velocity as a function of the rotational Reynolds number Re_ϕ.

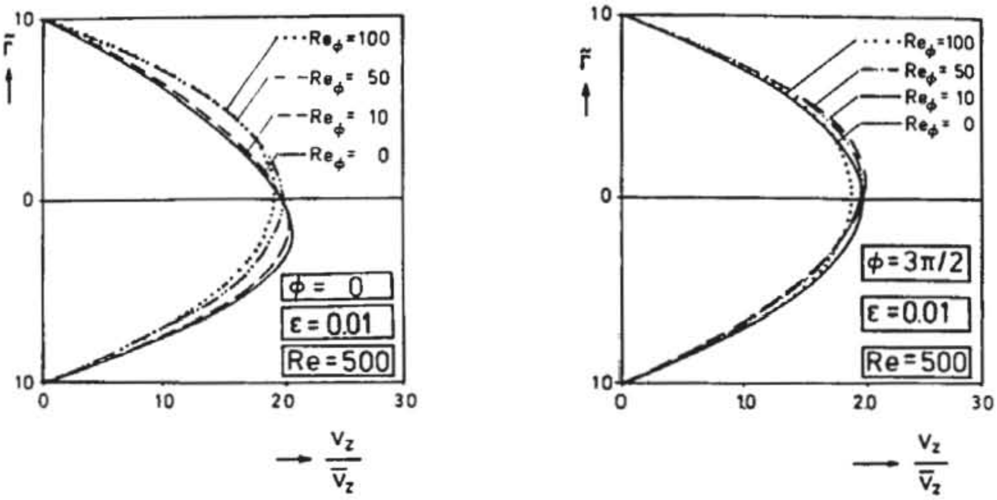

FIG. 10. Axial velocity as a function of the rotational Reynolds number Re_ϕ.

flow becomes more dominant. For $Re_\phi \geqslant 50$ the free convection effects have disappeared and there exists an almost rigid body rotation. The same effect can be observed in Fig. 9, where the radial velocity is plotted for different Re_ϕ in a vertical plane. With an increasing rotational speed the radial velocity decreases.

In Fig. 10 the axial velocity distribution in a vertical and a horizontal plane is plotted with the rotational Reynolds number Re_ϕ as a parameter. For small rotation velocities ($Re_\phi \leqslant 10$) the free convection effect on the axial velocity below the tube centreline, can be clearly detected to be a displacement of the velocity maximum in the vertical plane. With increasing Re_ϕ the velocity maximum shifts towards the 'eye' of the vortex, since fluid particles are transported from the tube centre to this region (compare with Fig. 7, $Re_\phi = 40$). If Re_ϕ increases further, the velocity maximum shifts back to the tube centre. However, the maximum value is smaller than that without rotation, which is a consequence of the destabilizing, turbulence exciting mechanism of rotation (see Section 2).

In Fig. 11 the effect of the ratio $\varepsilon = Gr/Re^2$ on the axial velocity profile in a vertical and a horizontal plane is demonstrated for a constant Re_ϕ. In the vertical plane a displacement of the maximum velocity towards the 'eye' of the vortex with an increasing ε can be observed, as already demonstrated in Fig. 10 for moderate Re_ϕ.

4. CONCLUSIONS

In the first part of this paper the effect of rotation on velocity and temperature profiles, friction and heat transfer coefficients of a laminar pipe flow with forced convection was investigated. It was demonstrated, that the tube rotation causes a destabilization of the laminar flow, which becomes turbulent due to rotation.

In the second part of this paper the interaction between free convection effects and rotation is considered. For small heat flux densities perturbation calculations were performed, to obtain profiles of the axial, radial and tangential velocity distribution. The plots of the velocity profiles and the stream function demonstrated that the influence of free convection vanishes with increasing rotational Reynolds number, which could also be observed in experimental investigations.

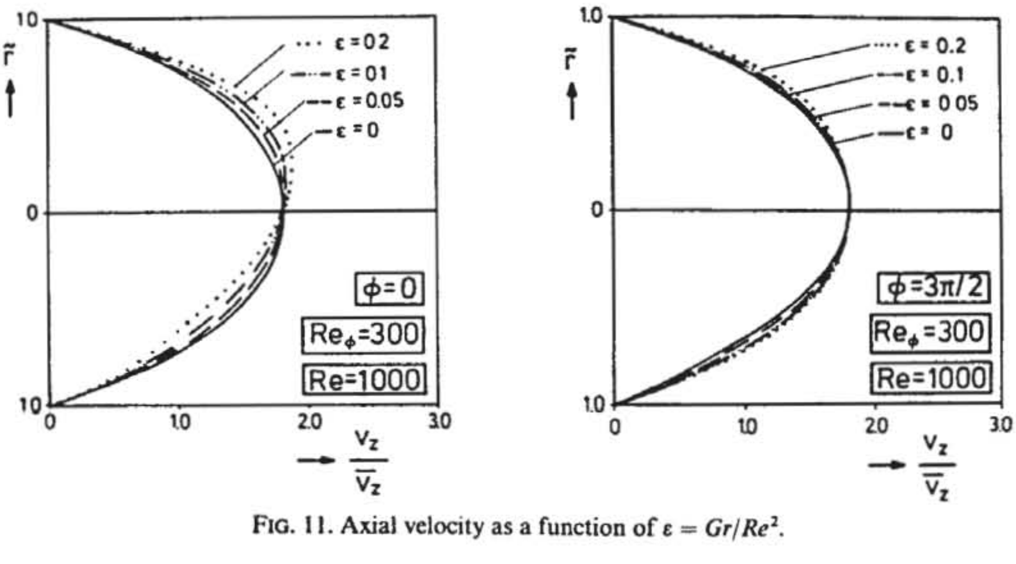

FIG. 11. Axial velocity as a function of $\varepsilon = Gr/Re^2$.

Acknowledgement—The support of this work by the Deutsche Forschungsgemeinschaft is greatly acknowledged.

REFERENCES

1. T. J. Pedley, On the instability of viscous flow in a rapidly rotating pipe, *J. Fluid Mech.* **35**, 97–115 (1969).
2. H. M. Nagib, Z. Lavan, A. A. Fejer and L. Wolf, Stability of pipe flow with superposed solid body rotation, *Physics Fluids* **14**, 766–768 (1971).
3. P. A. Mackrodt, Stability of Hagen–Poiseuille flow with superimposed rigid rotation, *J. Fluid Mech.* **73**, 153–164 (1976).
4. K. Kikuyama, M. Murakami, K. Nishibori and K. Maeda, Flow in an axially rotating pipe, *Bull. J.S.M.E.* **26**, 506–513 (1983).
5. G. Reich, Strömung und Wärmeübertragung in einem axial rotierenden Rohr, Doctoral Thesis, TH Darmstadt (1988).
6. B. R. Morton, Laminar convection in uniformly heated horizontal pipes at low Rayleigh numbers, *Q. J. Mech. Appl. Math.* **12**, 410–420 (1959).
7. E. Del Casal and W. N. Gill, A note on natural convection effects in fully developed horizontal tube flow, *A.I.Ch.E. Jl* **8**, 570–575 (1962).
8. K. Futayami and Y. Mori, Forced convection heat transfer in uniformly heated horizontal tubes—theoretical study, *Int. J. Heat Mass Transfer* **10**, 1801–1813 (1966).
9. G. Reich and H. Beer, Fluid flow and heat transfer in an axially rotating pipe—I. Effect of rotation on turbulent pipe flow, *Int. J. Heat Mass Transfer* **32**, 551–562 (1989).
10. A. F. Polyakov, Development of secondary free convection effects in forced turbulent flow in horizontal pipes, *J. Appl. Mech. Tech. Phys.* **5**, 632–637 (1974).

APPENDIX

$$D_1 = -2\frac{\dfrac{Re_\phi}{2i}D_5 + 2\left(\dfrac{Re_\phi}{2i}\right)^2 D_6}{J_1'\left(\sqrt{\left(\dfrac{Re_\phi}{2i}\right)}\right) - \sqrt{\left(\dfrac{2i}{Re_\phi}\right)}\,J_1\left(\sqrt{\left(\dfrac{Re_\phi}{2i}\right)}\right)}$$

$$D_2 = D_3 = 0$$

$$D_4 = -\frac{Re_\phi}{2i}D_5 - \left(\frac{Re_\phi}{2i}\right)^2 D_6 - D_1\sqrt{\left(\frac{2i}{Re_\phi}\right)}\,J_1\left(\sqrt{\left(\frac{Re_\phi}{2i}\right)}\right)$$

$$D_5 = -\frac{Re}{16}m_1\left(\frac{2i}{Re_\phi}\right)^{5/2} + Re\,m_2\left(\frac{2i}{Re_\phi}\right)^{7/2}$$

$$D_6 = -\frac{Re}{24}m_2\left(\frac{2i}{Re_\phi}\right)^{7/2}$$

$$d_{1R} = -2\frac{(d_{5I}+2d_{6I})\sum_{v=0}^{\infty}L_v(4v+2) + d_{5R}\sum_{v=0}^{\infty}K_v 4v}{\left(\sum_{v=0}^{\infty}K_v 4v\right)^2 + \left(\sum_{v=0}^{\infty}L_v(4v+2)\right)^2}$$

$$d_{1I} = -2\frac{(d_{5I}+2d_{6I})\sum_{v=0}^{\infty}K_v 4v - d_{5R}\sum_{v=0}^{\infty}L_v(4v+2)}{\left(\sum_{v=0}^{\infty}K_v 4v\right)^2 + \left(\sum_{v=0}^{\infty}L_v(4v+2)\right)^2}$$

$$d_{4R} = -d_{1R}\sum_{v=0}^{\infty}K_v + d_{1I}\sum_{v=0}^{\infty}L_v - d_{5R}$$

$$d_{4I} = -d_{1I}\sum_{v=0}^{\infty}K_v - d_{1R}\sum_{v=0}^{\infty}L_v - d_{5I} - d_{6I}$$

$$d_{5R} = -4\frac{Re}{Re_\phi^2}m_2$$

$$d_{5I} = -\frac{1}{8}\frac{Re}{Re_\phi}m_1$$

$$d_{6I} = -\frac{1}{12}\frac{Re}{Re_\phi}m_2$$

$$K_v = \frac{(-1)^v\left(\dfrac{Re_\phi}{2}\right)^{2v}}{(2v)!(2v+1)!2^{4v+1}}$$

$$L_v = \frac{(-1)^v\left(\dfrac{Re_\phi}{2}\right)^{2v+1}}{(2v+1)!(2v+2)!2^{4v+3}}$$

$$B_1 = -2n_1\frac{Re}{Re_\phi}D_1$$

$$B_2 = -8in_2\frac{Re}{Re_\phi^2}D_1$$

$$B_3 = -2n_1\frac{Re}{Re_\phi}D_4$$

$$B_4 = 2i\,Re\,n_2\left(\frac{2i}{Re_\phi}\right)^2 D_4 + i\,Re\,n_1\frac{2i}{Re_\phi}D_5$$

$$B_5 = 2i\,Re\,n_2\left(\frac{2i}{Re_\phi}\right)^2 D_5 + i\,Re\,n_1\frac{2i}{Re_\phi}D_6$$

$$B_6 = 2i\,Re\,n_2\left(\frac{2i}{Re_\phi}\right)^2 D_6$$

$$E_1 = -\frac{Re_\phi}{2i}E_3 - \frac{1}{J_1\left(\sqrt{\left(\dfrac{Re_\phi}{2i}\right)}\right)}\left[\left(\sqrt{\left(\frac{Re_\phi}{2i}\right)}E_4 + \left(\frac{Re_\phi}{2i}\right)^{3/2}E_5\right)J_0\left(\sqrt{\left(\frac{Re_\phi}{2i}\right)}\right) + \sqrt{\left(\frac{Re_\phi}{2i}\right)}E_6 + \left(\frac{Re_\phi}{2i}\right)^{3/2}E_7 + \left(\frac{Re_\phi}{2i}\right)^{5/2}E_8 + \left(\frac{Re_\phi}{2i}\right)^{7/2}E_9\right]$$

$$E_3 = -\frac{8}{3}in_2\frac{Re}{Re_\phi^2}D_1$$

$$E_4 = -\frac{1}{2}i\,Re\,n_1\frac{2i}{Re_\phi}D_1$$

$$E_5 = -\frac{1}{3}i\,Re\,n_2\left(\frac{2i}{Re_\phi}\right)^2 D_1$$

$$E_6 = i\,Re\,n_1\frac{2i}{Re_\phi}D_4 - 8E_7$$

$$E_7 = 2i\,Re\,n_2\left(\frac{2i}{Re_\phi}\right)^2 D_4 + i\,Re\,n_1\frac{2i}{Re_\phi}D_5 - 24E_8$$

$$E_8 = 2i\,Re\,n_2\left(\frac{2i}{Re_\phi}\right)^2 D_5 + i\,Re\,n_1\frac{2i}{Re_\phi}D_5 - 96i\,Re\,n_2\left(\frac{2i}{Re_\phi}\right)^2 D_6$$

$$E_9 = 2i\,Re\,n_2\left(\frac{2i}{Re_\phi}\right)^2 D_6$$

$$e_{1R} = -\frac{1}{\left(\sum_{v=0}^{\infty}K_v\right)^2 + \left(\sum_{v=0}^{\infty}L_v\right)^2}\left[\left\{(e_{4R}+e_{5R})\sum_{v=0}^{\infty}K_v(4v+2)\right.\right.$$

$$-(e_{4I}+e_{5I})\sum_{\nu=0}^{\infty} L_\nu(4\nu+4)+e_{6R}+e_{7R}+e_{8R}\Bigg\}$$

$$\times \sum_{\nu=0}^{\infty} K_\nu + \Bigg((e_{4I}+e_{5I})\sum_{\nu=0}^{\infty} K_\nu(4\nu+2)+(e_{4R}+e_{5R})$$

$$\times \sum_{\nu=0}^{\infty} L_\nu(4\nu+4)+e_{6I}+e_{7I}+e_{8I}+e_{9I}\Bigg\}\sum_{\nu=0}^{\infty} L_\nu\Bigg]-e_{3R}$$

$$e_{1I} = -\frac{1}{\left(\sum_{\nu=0}^{\infty} K_\nu\right)^2+\left(\sum_{\nu=0}^{\infty} L_\nu\right)^2}\Bigg[\Bigg\{(e_{4I}+e_{5I})\sum_{\nu=0}^{\infty} K_\nu(4\nu+2)$$

$$+(e_{4R}+e_{5R})\sum_{\nu=0}^{\infty} L_\nu(4\nu+4)+e_{6I}+e_{7I}+e_{8I}+e_{9I}\Bigg\}$$

$$\times \sum_{\nu=0}^{\infty} K_\nu - \Bigg\{(e_{4R}+e_{5R})\sum_{\nu=0}^{\infty} K_\nu(4\nu+2)-(e_{4I}+e_{5I})$$

$$\times \sum_{\nu=0}^{\infty} L_\nu(4\nu+4)+e_{6R}+e_{7R}+e_{8R}\Bigg\}\sum_{\nu=0}^{\infty} L_\nu\Bigg]-e_{3I}$$

$$e_{3R} = -\frac{4}{3}\frac{Re}{Re_\phi}n_2 d_{1R}$$

$$e_{3I} = -\frac{4}{3}\frac{Re}{Re_\phi}n_2 d_{1I}$$

$$e_{4R} = \frac{Re}{Re_\phi}n_1 d_{1R}$$

$$e_{4I} = \frac{Re}{Re_\phi}n_1 d_{1I}$$

$$e_{5R} = \frac{2}{3}\frac{Re}{Re_\phi}n_2 d_{1R}$$

$$e_{5I} = \frac{2}{3}\frac{Re}{Re_\phi}n_2 d_{1I}$$

$$e_{6R} = -2\frac{Re}{Re_\phi}n_1 d_{4R}+\frac{16}{Re_\phi}e_{7I}$$

$$e_{6I} = -2\frac{Re}{Re_\phi}n_1 d_{4I}-\frac{16}{Re_\phi}e_{7R}$$

$$e_{7R} = -4\frac{Re}{Re_\phi}n_2 d_{4R}-2\frac{Re}{Re_\phi}n_1 d_{5R}+\frac{48}{Re_\phi}e_{8I}$$

$$e_{7I} = -4\frac{Re}{Re_\phi}n_2 d_{4I}-2\frac{Re}{Re_\phi}n_1 d_{5I}-\frac{48}{Re_\phi}e_{8R}$$

$$e_{8R} = -4\frac{Re}{Re_\phi}n_2 d_{5R}+\frac{96}{Re_\phi}e_{9I}$$

$$e_{8I} = -4\frac{Re}{Re_\phi}n_2 d_{5I}-2\frac{Re}{Re_\phi}n_1 d_{6I}$$

$$e_{9I} = -4\frac{Re}{Re_\phi}n_2 d_{6I}.$$

ECOULEMENT ET TRANSFER DE CHALEUR DANS UN TUBE EN ROTATION—II. EFFET DE LA ROTATION SUR UN ECOULEMENT LAMINAIRE

Résumé—Les effets de la rotation d'un tube horizontal sur la distribution de vitesse et de température ainsi que sur le coefficient de frottement et de transfer de chaleur d'un écoulement axial laminaire sont étudiés analytiquement. Nous montrons que la rotation du tube a un effet déstabilisant sur l'écoulement laminaire qui devient turbulent. Les cellules de convection naturelle dues au chauffage de la paroi disparaissent cependant avec l'augmentation de la vitesse de rotation du tube. La méthode de perturbation appliquée aux équations de base permet de montrer de facon significative cette disparition des cellules de convection naturelle.

STRÖMUNG UND WÄRMEÜBERTRAGUNG IN EINEM AXIAL ROTIERENDEN ROHR—II. DER EINFLUSS DER ROTATION AUF EINE LAMINARE ROHRSTRÖMUNG

Zusammenfassung—Der Einfluß der Rotation auf Geschwindigkeits- und Temperaturprofile, Reibungsbeiwert und Wärmeübergangszahl einer laminaren Rohrströmung wird theoretisch untersucht. Es wird gezeigt, daß die Rotation eine destabilisierende Wirkung auf die laminare Strömung ausübt, die aufgrund der Rotation umschlägt und turbulent wird. Die durch eine Beheizung der Rohrwand auftretenden natürlichen Konvektionszellen verschwinden jedoch mit einer zunehmenden Drehzahl des Rohres. Hierzu wird eine Störungsrechnung durchgeführt, mit deren Ergebnissen das Verschwinden der Konvektionszellen sehr anschaulich gezeigt werden kann.

ТЕЧЕНИЕ ЖИДКОСТИ И ТЕПЛОПЕРЕНОС В АКСИАЛЬНО ВРАЩАЮЩЕЙСЯ ТРУБЕ—II. ВЛИЯНИЕ ВРАЩЕНИЯ НА ЛАМИНАРНОЕ ТЕЧЕНИЕ В ТРУБЕ

Аннотация—Аналитически исследуется влияние вращения трубы на профили скорости и температуры, на коэффициент трения и на теплоперенос к ламинарному потоку жидкости в трубе. Показано, что вращение дестабилизирует ламинарно течение в трубе, которое переходит в турбулентное. Возникающие при нагреве стенок свободноконвективные вихри исчезают с увеличением скорости вращения трубы. С этой целью проведен расчет возмущенного движения, результаты которого наглядно демонстрируют исчезновение свободноконвективных вихрей.